Impact of Plasticity and Flexibility on Docking Results for Cytochrome P450 2D6: A Combined Approach of Molecular Dynamics and Ligand Docking

Jozef Hritz, Anita de Ruiter, and Chris Oostenbrink*

Leiden-Amsterdam Center for Drug Research, Section of Molecular Toxicology, Department of Chemistry and Pharmacochemistry, Vrije Universiteit, De Boelelaan 1083, 1081 HV Amsterdam, The Netherlands

Received August 8, 2008

Cytochrome P450s (CYPs) exhibit a large plasticity and flexibility in the active site allowing for the binding of a large variety of substrates. The impact of plasticity and flexibility on ligand binding is investigated by docking 65 known CYP2D6 substrates to an ensemble of 2500 protein structures. The ensemble was generated by molecular dynamics simulations of CYP2D6 in complex with five representative substrates. The effect of induced fit, the conformation of Phe483, and thermal motion on the accuracy of site of metabolism (SOM) predictions is analyzed. For future predictions, the three most essential CYP2D6 structures were selected which are suitable for different kinds of ligands. We have developed a binary decision tree to decide which protein structure to dock the ligand into, such that each ligand needs to be docked only once, leading to successful SOM prediction in 80% of the substrates.

Introduction

Cytochrome P450s (CYPs)[a] form a superfamily of heme−thiolate-containing proteins which play a crucial role in the metabolism of drugs and other xenobiotics.[1] CYPs generally detoxify potentially hazardous compounds, but in a number of cases nontoxic parent compounds are bioactivated into toxic metabolites or procarcinogens into the ultimate carcinogens. The human isoform cytochrome P450 2D6 (CYP2D6) constitutes only ∼2% of the hepatic CYPs but is responsible for the metabolism of 15−20% of currently marketed drugs.[2,3] CYP2D6 substrates and inhibitors are commonly characterized by a protonated basic nitrogen and an aromatic system, which are also common features in drugs addressing the central nervous or cardiovascular system.[4] Inhibition of CYP2D6 may easily lead to adverse drug−drug interactions. Large interindividual differences exist in CYP2D6 activity, due to gene multiplicity and genetic polymorphisms, emphasizing the need to include metabolism prediction early in the drug discovery process.[5,6] Early considerations of AMDET properties (absorption, metabolism, distribution, excretion, and toxicology) include attempts to model the CYP activity *in silico*.[7−9] For many years, structure-based approaches had to rely on homology models[10] until the first (apo) structure of the enzyme was published in 2006.[11]

Many CYPs seem to show a larger extent of active site plasticity and flexibility when compared to many other proteins. This may be explained from the ability of CYPs to bind and metabolize a large variety of substrates.[12,13] Even if standard docking approaches are quite reliable for less flexible proteins, special care has to be taken for proteins with very malleable active sites. This paper describes the impact of different kinds of flexibility of CYP2D6 on the prediction of the site of metabolism (SOM). We will describe strategies to incorporate the most essential structural variety into efficient ligand docking methods. We use a variant of ligand docking into an ensemble of protein structures generated by molecular dynamics (MD) simulations. This approach was introduced by Pang and Kozikovski in their docking study of huperzine A to 69 snapshots of a MD trajectory of acetylcholinesterase.[14] The rationale behind this approach is supported by recent advances in the description of ligand−protein binding. The traditional lock-and-key picture seems to be gradually replaced by a model in which an ensemble of protein conformations is described and a ligand selectively binds to the most appropriate shape of the binding site.[15,16]

In silico structure-based predictions of drug metabolism are usually considered to be made up of (1) the binding orientation of the substrate in the active site, placing the reactive group in close vicinity of the heme iron atom, and (2) the intrinsic reactivity of this group.[17,18] The relative importance of these two issues will differ between different CYPs. The substrate binding pose will play a crucial role for the tight binding site of CYP1A2 but seems to be less relevant for the large binding site of CYP3A4. Here we address the prediction of the site of metabolism (SOM) based on the most likely poses of substrates within the active site of CYP2D6. In particular, we will address the effects of protein plasticity and flexibility on such predictions. For this, many thousands of docking experiments are performed, based on which a small number of protein structures will be selected which are most optimal for SOM predictions.

The only available crystal structure of CYP2D6 is an apo structure, for which the crystallographers already observed that the active site is too small to fit known CYP2D6 substrates.[11] Also, other groups reported better results when docking into CYP2D6 structures refined from MD simulations with ligand bound.[19,20] The active site needs to be opened up, to accommodate a variety of substrates. This raises the questions how much the active site needs to be enlarged and, more importantly, if different substrates should be fitted into the same shape of the active site. Because of their versatile function in the metabolism of diverse compounds, CYPs are known to show large plasticity in their active sites, being able to accommodate many different substrates.[12] In this work, we distinguish three different kinds of protein flexibility.

* To whom correspondence should be addressed. Phone: +31 20 5987606. Fax: +31 20 5987610. E-mail: c.oostenbrink@few.vu.nl.

[a] Abbreviations: CYP, cytochrome P450; CYP2D6, cytochrome P450 isoform 2D6; EDR, (*R*)-3,4-methylenedioxy-*N*-ethylamphetamine; LPBS, ligand probing binding site method; MD, molecular dynamics; MMC, 7-methoxy-4-(aminomethyl)coumarin; PPD, (*R*)-propranolol; CHZ, chlorpromazine; TMF, tamoxifen; SOM, site of metabolism.

10.1021/jm801005m CCC: $40.75
Published on Web 11/11/2008

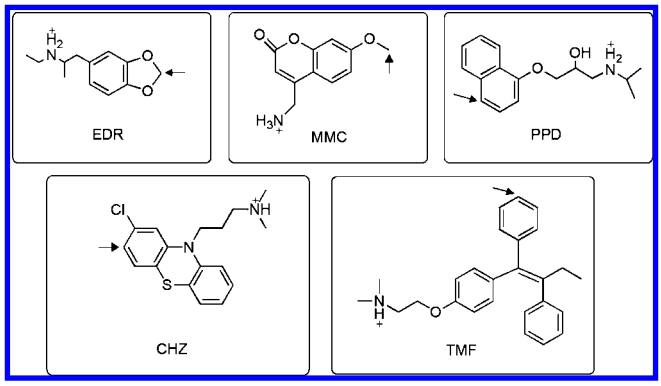

Figure 1. Chemical structures of the five representative substrates: (*R*)-3,4-methylenedioxy-*N*-ethylamphetamine (EDR), 7-methoxy-4-(aminomethyl)coumarin (MMC), (*R*)-propranolol (PPD), chlorpromazine (CHZ), and tamoxifen (TMF).

(1) Structurally different substrates will induce different conformations of the protein active site or, alternatively, specifically bind to different conformations from the overall structural ensemble of the protein.[16]

(2) Within the conformations suitable to accommodate a specific substrate, one may still distinguish different subclasses of conformations, which are separated by relatively high energetic barriers. In the case of CYP2D6 two such conformations are observed for the side chain of Phe483, as will be explained below.

(3) All atoms constituting the active site are continuously in thermal motion, leading to smaller fluctuations in the shape of the active site. We will show that also thermal fluctuations may have a strong effect on SOM predictions.

To incorporate these three types of plasticity and flexibility, we generate a library of 2500 protein structures, which covers the various conformations of the CYP2D6 active site. Subsequent docking experiments on all members of this library allows for an analysis of the effects of the different phenomena on the accuracy of SOM predictions. Finally, we will select the essential ensembles of protein structures and propose an optimal set of protein structures to be used in docking experiments. A simple decision tree model is also presented to select for any given putative substrate, which protein structure is most likely to yield an accurate SOM prediction.

Results

The library of protein conformations was built up in the following way. To account for induced fit effects, five representative substrates (Figure 1) were taken from a database of 65 known CYP2D6 substrates. Forty-five substrates could be grouped into five clusters, represented by the substrates in Figure 1. The remaining 20 substrates were placed in the sixth cluster. See Figure S1 in the Supporting Information for the complete set of substrates, how they are clustered, and an indication of the major SOM. We remark that for some substrates multiple SOMs were considered. One of the hypotheses to be investigated here is that the active site adopts a conformation around the representative substrates which is similar to the conformation it adopts around the other members of the cluster.

Opening of CYP2D6 Catalytic Site. Docking the smallest representative substrate (EDR) into the apo structure of CYP2D6 resulted in the SOM being placed at 4.5 Å from the heme iron. Subsequently, the system was solvated and electroneutralized by adding counterions and relaxed by molecular dynamics (MD) simulation. All waters, counterions, and EDR atoms were removed from the structure obtained after 100 ps of unrestrained MD, which was subsequently used for the docking of the larger representative substrate MMC. This procedure was repeated for the other representative substrates of increasing size (PPD, CHZ, TMF), thereby inducing CYP2D6 conformational changes to accommodate a wider range of substrates.

Phe483 Conformations. The largest conformational changes of the protein (mainly side chains) around the representative substrates occurred during the 100 ps of MD described in the previous paragraph. Subsequent MD simulations were performed to include thermal motions in equilibrium. If different conformations present at room temperature are separated by a low-energy barrier, then they should be adequately sampled within 0.5 ns of MD, but in the case of larger barriers the sampling within this time may be inadequate.

MD simulations of CYP2D6 in complex with each of the representative substrates revealed that two conformations of the Phe483 side chain are possible but that transitions take place on a time scale (~1 ns) that is too long to accurately determine the relative populations of these conformations. Therefore, we have performed 1 ns MD simulations for each of the representative substrates in which the χ_1 angle of Phe483 (χ_1^{483}) was restrained to either 70° or 170°. This leads to 10 structural ensembles of active site conformations, from each of which we stored 250 structures, sampled from the last 500 ps of the simulations. We refer to the ensembles by the name of the representative substrate used to generate them, followed by the approximate value of χ_1^{483}: EDR_170 represents the ensemble of 250 CYP2D6 structures which were obtained from MD of CYP2D6 in complex with EDR in which the dihedral angle χ_1 of the Phe483 side chain was restrained to 170°. The complete structural library now contains 2500 protein structures.

Docking into CYP2D6 Structural Ensembles. Sixty-five substrates of CYP2D6 with known sites of metabolism were docked into 250 protein structures for each of the 10 ensembles. An example of SOM prediction for the representative substrates for one particular docking simulation to one protein structure is shown under "single docking" in Table 1. This table presents the distance of the SOM from the heme iron atom (third column) for the first ranked pose (score in the fourth column).

As described in the Experimental Section, five docking simulations were performed for every protein structure, leading to the final prediction for one particular protein structure shown under "five dockings" in Table 1. It does not only show the SOM prediction (fifth column) but also the corresponding consensus between the five docking simulations (sixth column). These data were averaged over 250 CYP2D6 structures for every ensemble. The columns labeled as "250 frame ensemble" in Table 1 present for each representative substrate the fraction of frames for which the binding mode was predicted with the SOM within 6 Å from the heme iron atom. The same percentages for all 65 substrates docked into the PPD_70 ensemble giving the most reliable SOM prediction (as shown below) are presented in Figure 2. This figure is divided into six parts; the first five parts of the table contain the substrates belonging to clusters characterized by the listed representative ligands. Ligands which do not belong to any of these five clusters are listed in the sixth part of the figure. Tables with the same statistical analysis extended with consensus results for the highest ranked pose, over the five highest ranked poses, and over all 10 docking poses for all 10 ensembles are available in the Supporting Information (Tables S1−S10). For all 10 ensembles we note that the average reliability of binding mode prediction selecting the binding pose with the highest score from five independent dockings (third column, labeled "first rank") is slightly higher than the average

Table 1. Best Scored Results from One Particular Docking Simulation, Final Prediction Based on Five Independent Docking Simulations into the Last Frame, and Averages over the Complete PPD_70 Ensemble of CYP2D6 Structures, Showing Only the Five Representative Substrates

		single docking[c]		five dockings[f]		250 frame ensemble[i]	
code[a]	name[b]	dist[d]	score[e]	dist[g]	perc[h] (%)	first rank[j] (%)	consens[k] (%)
EDR	*R*-MDEA	3.5	24.4196	3.5	80	52.0	53.5
MMC	MAMC	3.5	26.7666	3.9	100	98.0	98.1
PPD	(*R*)-propranolol	4.6	36.1397	3.2	100	99.2	98.2
CHZ	chlorpromazine	3.5	41.9164	3.5	100	31.2	39.8
TMF	tamoxifen	3.3	42.7726	3.7	100	86.4	86.6
total[l]		46/65		44/65	70.2	62.0	61.8

[a] Three letter code for the substrate. [b] Name of the substrate. [c] First ranked docking pose over 10 poses from a single docking simulation. [d] Distance from the SOM to the heme iron in the first ranked docking pose. [e] Value of the Chemscore docking score for the first ranked pose. [f] Results based on five independent dockings into the same frame. [g] Distance from the SOM to the heme iron in the best ranked docking pose over all 50 poses. [h] Fraction of the first ranked poses in individual dockings (10 poses) giving the same SOM prediction as the overall best ranked pose. [i] Results based on five independent dockings into the ensemble of 250 frames. [j] Percentage of frames (over 250 frames) where the highest scored binding pose (over five docking simulations; 50 poses) places the SOM within 6 Å distance from the heme iron atom. [k] Same percentage as in footnote *j*, averaged over the first ranked poses of all docking simulations. [l] Statistics for all 65 substrates; number of substrates for which the SOM was predicted within 6 Å from the heme iron for the best scoring pose in one docking simulation, over five docking simulations; the last three columns are averages over corresponding columns.

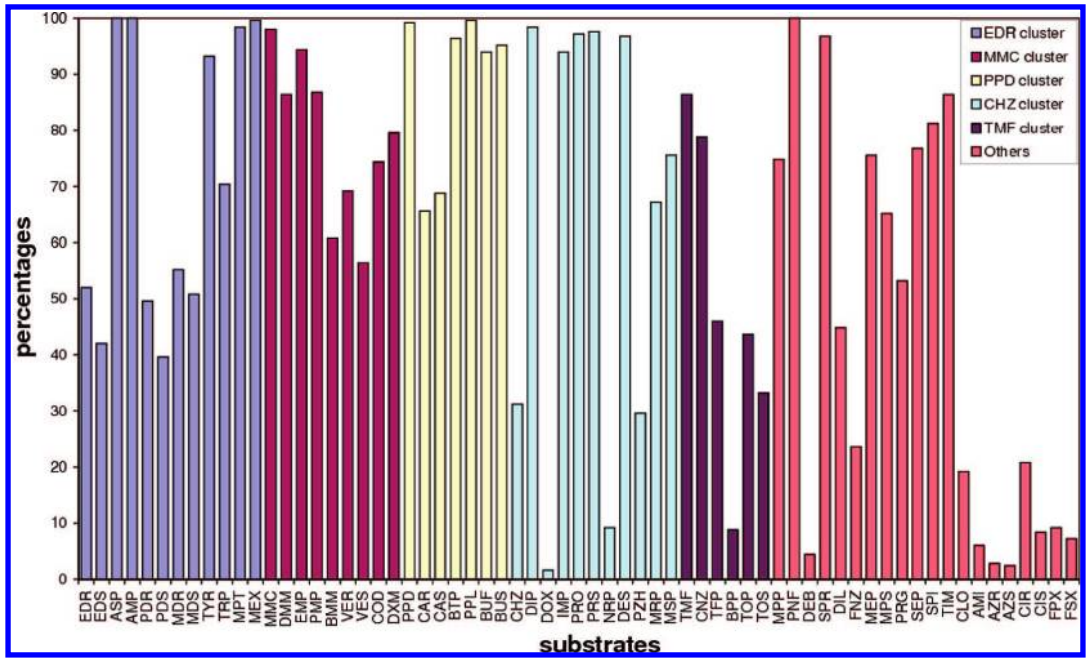

Figure 2. Percentage of frames within the PPD_70 ensemble in which the highest scored binding pose (over five docking simulations) places the SOM within 6 Å distance from the heme iron atom. Chemical structures and names of all 65 substrates corresponding to the three letter codes are listed in Figure S1 (a−f) and Tables S1−S10, respectively, in the Supporting Information. Substrates are divided into six groups according to five clusters named by representative substrates, indicated with different colors in this figure.

over all first ranked poses of the individual dockings (fourth column, labeled "consens").

Discussion

The structural ensemble of CYP2D6 covers a wide range of active site plasticity and flexibility. The effect of thermal motion, induced fit, and the conformation of Phe483 on the reliability of the SOM prediction is discussed in the following sections.

Impact of Thermal Fluctuations on CYP2D6 Docking Predictions. Figure 3 shows the variation in the number of substrates for which the first ranked pose places the SOM within 6 Å distance from the heme iron atom for the PPD_70 ensemble. A sampling time of 2 ps between subsequent structures allows for only small conformational changes. Still, it can be seen that even such small changes in the protein structure have an impact on the SOM prediction. For most ensembles the deviations from the average values (summarized in Table 2) are within 10%, but more extreme fluctuation can be observed. For instance, in the EDR_70 ensemble, the percentage of substrates that is correctly placed in the active site changes from 0% in structure 239 (indicated as EDR_70_fr_239) to 41.5% in the next structure (EDR_70_fr_240). We do not see any obvious structural difference between these protein structures (Figure 4), which indicates that very subtle differences in protein structures can have tremendous effects on the SOM prediction. In Figure 4, we show the binding mode prediction for substrate MMC into both frames, which demonstrates the observation that many substrates are bound to a subpocket between Gln244 and Ala300 when docked to the EDR_70_fr_239 structure. It seems that such erratic behavior in the pose predictions can be traced to the fact that the scoring functions are not continuous, so that small structural changes can have big effects on the prediction of the scores. We also emphasize that a correct inclusion of entropic effects would prevent rare events from becoming the first ranked predictions. This example demonstrates the risk of blindly selecting a single protein structure and strengthens us in the belief that one should consider the values that are averaged over the structural ensemble (last two

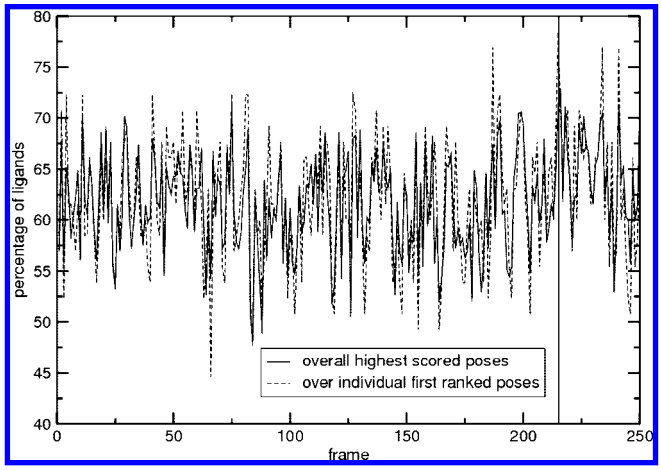

Figure 3. Docking into individual frames of the PPD_70 ensemble of CYP2D6 structures. Solid line: The fraction of substrates for which the binding pose with the overall highest score (from five docking simulations) positions the SOM within 6 Å from the heme iron atom. Dashed line: The average value when considering the first ranked poses for individual docking simulations separately. Frame 216 (indicated by the vertical line) was finally taken as the single CYP2D6 structure giving the highest docking prediction reliability.

Table 2. Average Percentage over All Structures and 65 Substrates for Each of the 10 Generated Ensembles

	CYP2D6/ EDR (%)	CYP2D6/ MMC (%)	CYP2D6/ PPD (%)	CYP2D6/ CHZ (%)	CYP2D6/ TMF (%)
$\chi_1^{483} \approx 70°$	45.4	42.2	62.0	57.4	47.4
$\chi_1^{483} \approx 170°$	48.6	48.2	62.0	59.6	51.4

columns of Table 1 and Tables S1−S10) or make a careful selection of single frames as shown below.

Impact of Induced Fit Effects on CYP2D6 Docking Predictions. Table 3 presents the ligand−probe binding site (LPBS) distance (see Experimental Section) between the 10 structural ensembles, based on the percentages of correct predictions in Tables S1−S10. The largest difference of 36% is observed between the MMC_70 and PPD_70 ensembles. Different structural ensembles obtained from simulations of different representative substrates are not equally well able to accommodate the various substrates. This can be seen from the percentage of frames in which individual substrates are positioned with their SOM within 6 Å from the heme iron atom (Tables S1−S10). We can determine if a substrate is indeed most often correctly placed in the ensemble generated for the representative substrate of the cluster to which it belongs. Table 4 shows how the percentages of protein structures in which a correct pose was predicted for the representative substrates docked into all ensembles. It can be seen that for MMC, PPD, and CHZ we indeed obtain the highest reliability when docking into protein structures refined from MD of CYP2D6 in complex with themselves. For TMF a higher reliability (∼90%) is obtained when docking into the CHZ_170 ensemble. Still, the TMF_70 ensemble itself also leads to a quite high reliability (∼70%). On the other hand, the reliability of docking EDR into the EDR_70 and EDR_170 ensembles is significantly lower (<40%) than when docking to the PPD_170 ensemble (∼63%).

Table 4 also shows that one of the most promiscuous substrates is MMC because a high reliability is obtained when docking to most of the structural ensembles. On the other hand, E-doxepine seems to be very sensitive to the shape of the protein binding site. Successful binding poses were only obtained to a significant level (70%) when it was docked into the MMC_70 ensemble.

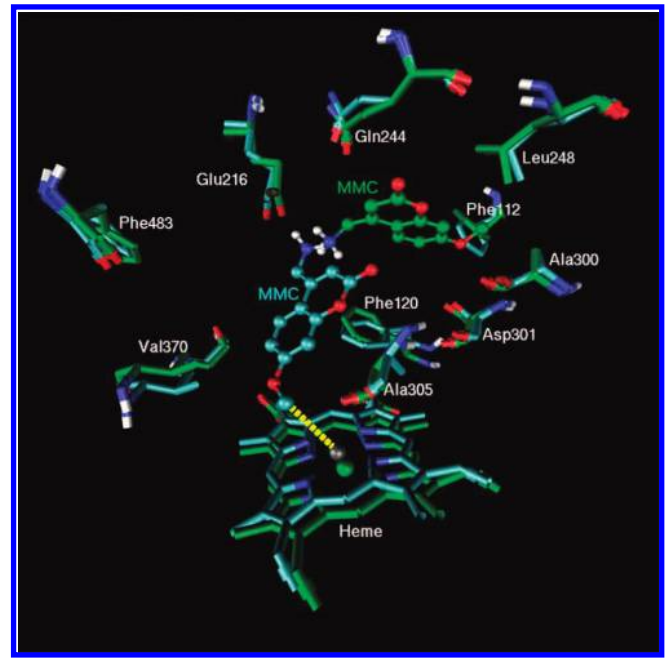

Figure 4. Binding mode prediction for MMC (ball and stick) when docked into the EDR_70_fr_239 structure (shown in green) and in the very similar EDR_70_fr_240 structure (shown in cyan). No successful correct poses were observed for any of 65 substrates in the green structure, but many occupy a subpocket between Gln244 and Ala300. In the cyan structure 27 substrates docked with the SOM within 6 Å from heme iron (indicated by the yellow dashed line).

Impact of the Conformation of Phe483 on CYP2D6 Docking Predictions. From the ensemble tables (Tables S1−S10) and from Table 4, it can be seen that substrates show different sensitivity toward the side-chain conformation of Phe483. The most significant difference is observed for substrates belonging to the MMC cluster, which are significantly more often placed correctly in the MMC_170 ensemble than in the MMC_70 ensemble (Table 5). A closer inspection revealed that Phe483 with $\chi_1^{483} \approx 170°$ does not stabilize the correct binding poses but rather destabilizes the incorrect binding pose (Figure 5). It is interesting to note that an experimental study on the effect of the F483A mutation on the metabolism of four substrates shows the largest effect for MMC. The F483A mutant does not show any metabolism of this substrate anymore.[21] The molecular explanation of this observation may very well be that the mutant binds MMC in binding poses similar to the not catalytically active pose (green) in Figure 5, as this is no longer destabilized by Phe483.

Essential Conformational Ensembles. The 65 CYP2D6 substrates can be reclustered according to the ensemble of structures that accommodates them most often in catalytically active poses (Table S11 in the Supporting Information). This reclustering shows that, for almost all substrates, at least one ensemble exists that correctly predicts the SOM with high reliability, leading to an overall reliability of 75.4%. We also investigated which are the essential conformational essembles; i.e., how many ensembles should be included to approach the value of 75.4%. Table 2 presents the average reliability over all substrates when considering single ensembles. The ensemble leading to the largest number of substrates with their SOM within 6 Å from the heme iron atom are the PPD_70 and the PPD_170 ensemble (∼62%), followed by the CHZ_170 and the CHZ_70 ensemble (∼58%). Because these are averages over 250 protein structures and over 65 substrates, the conformation of Phe483 has only a small effect on these percentages. Next,

Table 3. Ligand-Probed Binding Site (LPBS) Distance between the 10 Protein Ensembles[a]

	EDR_70 (%)	EDR_170 (%)	MMC_70 (%)	MMC_170 (%)	PPD_70 (%)	PPD_170 (%)	CHZ_70 (%)	CHZ_170 (%)	TMF_70 (%)	TMF_170 (%)
EDR_70	0	9.3	17.1	17.3	30.3	28.4	26.7	26.8	21.7	20.6
EDR_170		0	18.4	17.1	28.1	24.7	24.6	23.5	20.7	18.0
MMC_70			0	23.0	36.0	33.5	29.6	30.8	21.6	23.3
MMC_170				0	27.2	29.4	30.3	30.4	25.2	23.1
PPD_70					0	16.0	26.5	26.8	30.8	27.6
PPD_170						0	18.4	18.0	27.9	21.7
CHZ_70							0	10.9	26.8	18.0
CHZ_170								0	26.5	16.3
TMF_70									0	21.0
TMF_170										0

[a] For a description of the LPBS distance, see the Experimental Section.

Table 4. Fraction of Structures for Which the Substrates Dock Correctly into the Different Structural Ensembles[a]

CYP2D6 ensemble	EDR (%)	MMC (%)	PPD (%)	CHZ (%)	TMF (%)	E-doxepine[b] (%)
EDR_70	36.8	58.8	40.4	56.0	41.2	10.0
EDR_170	39.6	78.0	39.2	36.8	37.6	18.4
MMC_70	16.0	59.6	62.8	62.0	9.2	**70.0**
MMC_170	29.2	**98.4**	50.0	39.6	63.2	5.2
PPD_70	52.0	98.0	**99.2**	31.2	86.4	1.6
PPD_170	**62.8**	97.2	97.6	78.8	60.4	0.4
CHZ_70	62.4	74.0	91.2	98.0	52.4	0.4
CHZ_170	60.8	95.6	86.0	**100.0**	**90.4**	0.0
TMF_70	6.8	71.6	96.0	4.0	65.2	4.8
TMF_170	41.2	85.2	84.0	86.0	70.0	1.6

[a] A docking pose is considered to be correct if the SOM of the substrate is placed within 6 Å of the heme iron atom. [b] E-doxepine is the substrate which is the most sensitive to the structural ensemble to which it is docked.

Table 5. Effect of the Phe483 Side-Chain Conformation on the Fraction of Structures for Which the Substrates Dock Correctly into Ensembles of Structures[a]

code[b]	name[c]	MMC_70 (%)	MMC_170 (%)
MMC	MAMC	59.6	98.4
DMM	diMAMC	30.4	93.2
EMP	EMAMC	45.2	90.4
PMP	PMAMC	39.2	67.6
BMM	BMAMC	27.2	55.6
VER	(*R*)-venlafaxine	8.8	24.0
VES	(*S*)-venlafaxine	7.2	18.0
COD	codeine	3.2	13.6
DXM	dextromethorphan	18.4	76.4
average%		26.6	59.7

[a] A docking pose is considered to be correct if the SOM of the substrate is placed within 6 Å of the heme iron atom; data shown for the substrates belonging to the MMC cluster where the strongest effect was observed only. [b] Three letter code of the substrate. [c] Name of the substrate.

we have analyzed all combinations of two and three ensembles and select for every substrate the ensemble for which the highest value was obtained. This gives an upper limit to the averaged reliability over all substrates. The combinations with the best overall prediction are given in Table 6, with the optimal reliability given in the third row. The assignment of the substrates to the ensembles for all combinations is available in Table S12 of the Supporting Information. The upper bound to the SOM predictions converge to the overall upper bound based on ensembles of 75.4%, with a value of 72.3% when including only three ensembles. Note that even though all combinations of ensembles were considered, the optimal combinations always contain the same ensembles as the combination formed with one ensemble less (Table 6).

For almost all substrates there is at least one structural ensemble for which the SOM prediction is quite good. The only exceptions are (*R*)- and (*S*)-fluoxetine with a maximum reliability of only ~8%. These substrates show a trifluoro group

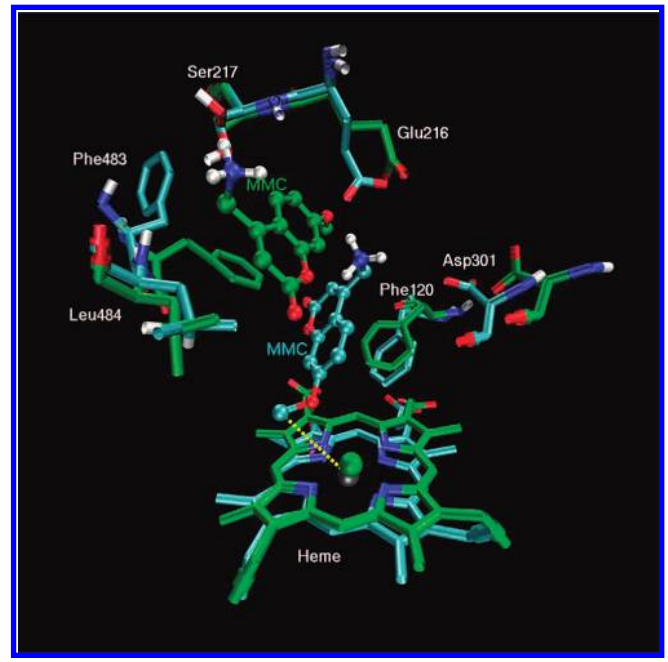

Figure 5. The number of frames into which MMC is incorrectly docked is significantly higher for the MMC_70 ensemble (40.4%) (in green) than for the MMC_170 ensemble (1.6%) (in cyan). The side chain of Phe483 with $\chi_1^{483} \approx 170°$ seems to destabilize the incorrect binding mode.

and have their SOM at the positively charged nitrogen atom. For most CYP2D6 substrates the positively charged nitrogen atom is expected to interact with the negatively charged side chain Glu216 (see, e.g., Figures 4 and 5), and the major SOM is elsewhere in the molecule. This is also the case for the five representative substrates used in this study. However, there are also CYP2D6 substrates following different binding modes (e.g., substrates metabolized close to the positively charged nitrogen atom (N^+)) which would not be found if one would constrain the Glu216−N^+ distance during docking simulation. For all substrates that are metabolized close to the positively charged nitrogen atom, other than (*R*)- or (*S*)-fluoxetine, there is at least one ensemble that still shows a reasonable SOM prediction. In most cases, this is the TMF_70 ensemble, in which the active site was opened up most, allowing the substrate to dock in a larger variety of poses. The fact that successful ensembles are found for most substrates indicates that the CYP2D6 structural library is extensive enough to dock substrates that are quite distinct from the representative substrates.

Correlation of Molecular Properties with Essential Conformational Ensembles. The observation that the reliability of SOM predictions can be as high as 72.3%, using only three structural ensembles, is promising, but it is far from trivial to

Table 6. Percentage of Correctly Docked Substrates for Essential Groups of Ensembles and Single Structures[a]

essential groups	1	2	3	all
ensembles[b]	PPD_70	PPD_70 CHZ_170	PPD_70 CHZ_170 TMF_70	all 10 ensembles
optimal reliability[c] (%)	62.0	70.3	72.3	75.4
reliability based on decision tree[d] (%)	62.0	63.6	64.2	
single structures[e]	PPD_70_fr_216	PPD_70_fr_216 CHZ_170_fr_79	PPD_70_fr_216 CHZ_170_fr_79 TMF_70_fr_3	65 structures
optimal reliability[f] (%)	71.3	86.2	89.8	100
reliability based on decision tree[g] (%)	71.3	79.4	80.3	

[a] A docking pose is considered to be correct if the SOM of the substrate is placed within 6 Å of the heme iron atom. [b] Sets of the essential ensembles. [c] Maximum reliability over 65 substrates where for each substrate the optimal value toward the ensembles in the given set is taken. [d] Averaged reliability over 65 substrates where for each substrate the ensembles are selected based on the decision tree in Figure 6. [e] Sets of the essential structures. [f] Maximum reliability over 65 substrates where for each substrate the optimal value toward the structures in the given set is taken. [g] Averaged reliability over 65 substrates where for each substrate the structures are selected based on the decision tree in Figure 6.

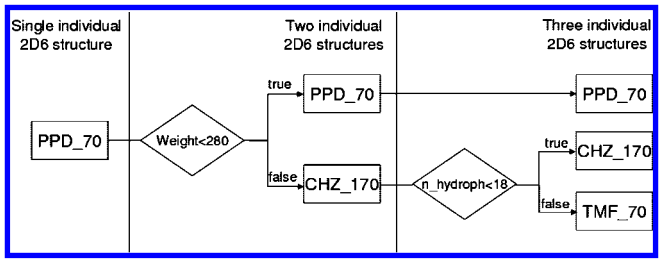

Figure 6. Binary decision tree using the molecular weight and the number of hydrophobic atoms to separate substrates into two or three groups corresponding to different individual structures or ensembles. This way, the optimal ensemble or single protein structure can be selected for a substrate *a priori*.

determine *a priori* to which ensemble a ligand should be docked. PPD-like compounds are best docked to the PPD_70 ensemble, and CHZ-like compounds are best docked to the CHZ_170 ensemble, but there are also some stereoisomers that give better results when docked to the PPD_70 ensemble. As noted before, the TMF_70 ensemble seems most suited for substrates which are (atypically) metabolized close to the protonated nitrogen.

For new, possibly more diverse, sets of compounds it would very advantageous if general molecular descriptors could be used to predict the optimal ensemble of protein structures. Binary decision trees were developed to divide the substrates over two (PPD_70 and CHZ_170) or three (PPD_70, CHZ_170, TMF_70) ensembles. The molecular weight was found to be the most important descriptor to determine if substrates should be docked into the PPD_70 or the CHZ_170 ensemble. A further improvement of the overall reliability can be obtained, including the TMF_70 ensemble and using the number of hydrophobic atoms to divide the substrates between the CHZ_170 and TMF_70 ensembles. This decision tree is schematically drawn in Figure 6, and the average number of successful SOM predictions following this decision tree is given in the fourth row of Table 6. Note that the increase in these values is considerably lower than the upper bounds to the predictions discussed in the previous section, which shows that the separation according to the decision tree is still quite far from the optimal one.

Single Frames with the Highest Reliability of Prediction. The previous sections describe the selection of essential CYP2D6 ensembles to dock substrates with a high reliability. For many applications, such as virtual screening of large compound libraries, it is not possible to perform docking into complete structural ensembles. Therefore, it is of enormous practical interest to select only very few protein structures, which lead to accurate SOM predictions. To find the single CYP2D6 structure that offers the best SOM predictions, we first selected from the library of 2500 structures the 15 protein structures with the highest fraction of correct SOM predictions. Two additional docking simulations (each of five docking runs) were performed for these structures, to obtain a higher consensus between the different runs. Two single frames were found in which >71% of the substrates docked correctly. These originated from the PPD_70 ensemble (structure 216: PPD_70_fr_216) and from the PPD_170 ensemble (structure 173: PPD_170_fr_173).

The fact that a single structure can be selected is extremely important if one wishes to perform docking experiments for many putative inhibitors or substrates and no specific knowledge is available for the ligand. These two structures offer the most reliable docking poses out of all 2500 available protein structures even though we note that these structures are only slightly better than the 15 initially selected protein structures. We stress that it is important to select protein structures carefully. As was mentioned above, docking into the EDR_70_fr_239 structure did not position the SOM of any substrate within 6 Å of the heme iron atom within the first ranked pose. The choice of the optimal structures will depend on the docking protocol and scoring function that is used. It is unlikely that when using, e.g., a different docking program this protein structure will fail completely, but different structures may perform slightly better.

We compare the single protein structures that were selected here to a homology model that was developed several years ago in our group.[10,22] The 65 substrates were docked to this model using the same settings as before, and for 60% of the substrates the SOM was placed within 6 Å of the heme iron atom for the first ranked pose. This is significantly lower than the 71% obtained here for the newly refined structures. When docking directly to the original apo crystal structure of CYP2D6, this percentage is only 20%. Using CYP2D6 structures from a MD simulation starting from this apo structure without adding a substrate decreases the reliability of SOM predictions to 0−9%, depending on the chosen frame (data not shown).

Essential Single Protein Structures. Similar to what was described for the ensembles, we can search for a small set of essential single protein structures. The single structures selected in the previous section represent an essential set of size 1. Sets of two and three single protein structures were selected from the 2500 structures as well and are given in the fifth row of Table 6. For the combination of three structures, an exhaustive search involves searching through 2500^3 combinations. Rather, we have limited our search to sets of three structures that contain the set of two optimal protein structures. From an exhaustive search, this set already contains the PPD_70_fr_216 structure, which is the best single structure. The sixth row of Table 6 gives an upper bound to the docking reliability when using these

sets of structures, by selecting for every substrate an optimal structure. Table S13 in the Supporting Information specifies for each of these sets which substrate is best docked in which protein structure. Note that the essential single structures stem from the essential ensembles determined earlier, although this was not imposed in the search algorithm. Therefore, it is not so surprising that the binary classification tree that was developed to divide the substrates over the single protein structures is the same as the one described for the essential ensembles (Figure 6). The seventh row of Table 6 presents the reliability in the docking predictions, which increases from 71.3% for a single structure to 79.4% and 80.3% when taking two or three structures into account, respectively. This increase is significantly higher than observed for the essential ensembles (fourth row of Table 6). We stress that these values can be obtained without any additional increase of computational demands as compared to docking into a single protein structure, as every substrate is docked only once to a protein structure selected based on the decision tree (Figure 6).

On the other hand, if substrates are docked to all three essential protein structures, the consensus between predictions can be used. The reliability of the binding mode prediction is 90% if the best frame is selected for every substrate. This means that if substrates are docked to all three structures, and we obtain the same binding mode, one can be almost sure that it will be correct. From the 65 substrates, 29 showed complete consensus when docking to the three essential structures. For 23 of these, the SOM is within 6 Å from heme iron atom. Two of the remaining six substrates are (*R*)- and (*S*)-fluoxetine, which were already described above as failing to dock in the majority of the 2500 protein structures. Among the 29 substrates, there are 11 substrates for which the consensus between the five individual docking runs (second part of Table 1) was 100%. All of these have the SOM within 6 Å from the heme iron atom. In cases where no consensus is reached between the different protein structures, we recommend to consider the two or three docking poses for further analysis (one of them is most likely correct). As mentioned earlier, if the substrate is docked to the TMF_170_fr_3 structure and places a charged nitrogen close to the heme iron atom, this docking pose deserves attention, even if such poses are not observed for the other two protein structures.

Conclusions

Structural refinements were performed on the crystal structure of cytochrome P450 2D6 (CYP2D6). The active site in this apo structure is too small to be used directly for predictions of the site of metabolism (SOM) in substrates (only 20% reliability), so we have adopted the active site to five representative substrates. Ten structural ensembles of 250 protein structures each were generated using molecular dynamics (MD) simulations of CYP2D6 in complex with each of the five representative substrates, in which two different conformations of the side chain of Phe483 were considered ($\chi_1^{483} \sim 70°$ and $\chi_1^{483} \sim 170°$). Docking experiments were performed for 65 substrates into all 2500 protein structures. Statistical analysis of the obtained docking poses revealed that even though thermal motion generally involves only small conformational changes, these may have a dramatic effect on the resulting docking poses. This strongly warns against performing docking experiments on any single (MD) protein structure and rather suggests to consider averages over structural ensembles or carefully selected protein structures only.

The effect of the side-chain conformation of Phe483 was seen to be strongest for the cluster of substrates represented by MMC. We suggest that Phe483 destabilizes substrate orientations far away from the heme iron, in accordance with site-directed mutagenesis data. The ensembles obtained from MD of CYP2D6 in complex with PPD and CHZ display the highest number of substrates with their SOM placed within 6 Å from the heme iron atom in the first ranked pose. The ensembles PPD_70, CHZ_170, and TMF_70 were determined to be the most essential ones.

These ensembles may be used for SOM prediction, but it is probably computationally too demanding to screen large databases for putative inhibitors or ligands by docking into complete ensembles. Therefore, we have selected a single CYP2D6 structure (PPD_70_fr_216) which offers a SOM prediction reliability of 71%. This reliability can be theoretically further increased up to 90% if part of the substrates are docked into the CHZ_170_fr_79 and TMF_70_fr_3 structures. A simple and robust decision tree was developed increasing the SOM prediction reliability to 80% without any additional computational costs. This offers a very powerful tool to perform SOM predictions efficiently, where every compound needs to be docked to one protein structure only.

The effects that we described here are not only valid for CYPs but are highly relevant for a much wider range of proteins. The large sensitivity of docking reliability not only due to larger conformational changes but also due to thermal motion should be kept in mind in any docking experiment, regardless of the protein target. Also, we have suggested techniques to open the binding site of apo structures and to select the most appropriate structures for high-throughput docking experiments. These findings are relevant for docking studies on any protein target.

Experimental Section

Clustering and Selection of Representative Substrates. A set of 65 known substrates of cytochrome P450 2D6 that was previously used in docking experiments was taken from the literature.[22] These substrates were clustered based on their expected binding mode. We assume that a conformation of the CYP2D6 active site that accommodates one representative substrate will also be able to accommodate the other substrates from the same cluster. Clustering was based on the observation that most substrates contain a positively charged nitrogen in a flexible tail, connected to a rigid body, usually consisting of several aromatic rings. The width of the substrates perpendicular to the flexible tail was used to cluster the compounds into five groups, according to Table S1 in the Supporting Information. The representative substrates for these five clusters are given in Figure 1. Twenty substrates could not be assigned to any of these clusters.

CYP2D6 Structure Preparation. The crystal structure of CYP2D6[11] was downloaded from the Protein Data Bank (www.pdb.org; code 2F9Q). We selected chain A of this apo structure, in which some atoms of a few side chains were missing. These were modeled using the program MOE.[23] Three mutations required for the crystallization were reverted to the wild-type amino acids (Asp230Leu, Arg231Leu, and Met374Val). Coordinates for the missing loop between amino acids 42 and 51 were taken from an earlier homology model.[10] Atoms for which new coordinates were assigned were minimized and equilibrated for 10 ps of molecular dynamics (MD) simulation at 300 K, while position restraints were assigned to the rest of the protein structure.

Molecular Dynamics Simulations. Molecular dynamics simulations of CYP2D6 in complex with the five representative substrates (EDR, MMC, PPD, CHZ, TMF) were performed using the GROMOS05 simulation package[24] in combination with the GROMOS 45A4 force field.[25,26] For every substrate two simulations of 1 ns were performed in which the χ_1 angle of the Phe483 was restrained to either 70° or 170° using a force constant of 30.0 kJ mol^{-1} deg^{-2}. All bonds were constrained, using the SHAKE

algorithm[27] with a relative geometric accuracy of 10^{-4}, allowing for a time step of 2 fs used in the leapfrog integration scheme.[28] The system was solvated in 20292 explicit SPC water molecules[29] and 7 Na^+ ions in a periodic rectangular simulation box. After a steepest descent minimization to remove clashes between molecules, initial velocities were randomly assigned from a Maxwell−Boltzmann distribution at 300 K, according to the atomic masses. The temperature was kept constant using weak coupling to a bath of 300 K with a relaxation time of 0.1 ps.[30] The CYP2D6−substrate complex and the solvent (including the ions) were independently coupled to the heat bath. The pressure was controlled using isotropic weak coupling to atmospheric pressure with a relaxation time of 0.5 ps.[30] Van der Waals and electrostatic interactions were calculated using a triple range cutoff scheme. Interactions within a short-range cutoff of 0.8 nm were calculated every time step from a pair list that was generated every five steps. At these time points, interactions between 0.8 and 1.4 nm were also calculated and kept constant between updates. A reaction field contribution was added to the electrostatic interactions and forces to account for a homogeneous medium outside the long-range cutoff, using the relative permittivity 61 of SPC water.[31]

Docking. From the last 500 ps of each of the 10 MD simulations described above, 250 structures were stored to disk. The GROMOS 45A4 force field is a united atom force field, meaning that aliphatic hydrogen atoms are treated implicitly. Coordinates for the implicit hydrogen atoms were added, all waters, counterions, and the representative substrates were removed, and the resulting files were converted into mol2 file format using Sybyl (version 6.8) and the standard Tripos atom and bond types for the amino acids and the heme group.

Docking was performed by GOLD (Genetic Optimization for Ligand Docking)[32] version 3.3.1 in combination with the Chemscore scoring function[33] parametrized for heme-containing proteins.[34] This scoring function outperformed the Goldscore scoring function in our preliminary work (data not shown). Ten docking runs with maximally 1000 genetic algorithm operations were performed using a population of 100 genes. The center point for the docking was placed in the middle of the cavity in between residues Phe120 and Phe483. The radius from this point was set to 18 Å to include the solvent channel in the accessible volume for the docking. We stress that a shorter radius will automatically result in predicted binding modes that are closer to the heme and thus positively bias the SOM predictions. No water molecules, or a sixth ligand on the heme iron atom, were taken into account.

Docking Reproducibility. Because the genetic algorithm used for docking utilizes a considerable amount of randomness, results from individual docking simulations (consisting of 10 runs) are not reproducible. For about 20% of substrates, the evaluation of the first ranked docking pose (see below) changed when two independent docking experiments were performed. Therefore, we have performed five independent docking experiments (10 docking runs each) for all 65 substrates in all 2500 protein structures. For every experiment 10 docking poses were obtained, and the SOM prediction was based on the first ranked pose. The final SOM prediction is subsequently based on the binding mode with the highest score over all 50 binding poses. Furthermore, we assigned a weight (sixth column in Table 1) for the prediction, based on the consensus with the prediction according to the other four first-ranked poses. Note that this approach is not the same as performing a single experiment with 50 docking runs, because the docking program explicitly searches for new solutions that differ from previous runs.

Analysis. Any docking pose of a substrate in a protein structure is considered to be correct if the known SOM is within 6 Å of the heme iron atom.[22] This relatively wide criterion accounts for thermal fluctuations and dioxygen binding. In order to use this criterion in predictions for new substrates, it is important that one only needs to consider the first ranked pose, which should correspond to the binding pose with the highest affinity. Unfortunately, scoring functions are often not accurate enough to correctly predict the first ranked pose. Also, the highest affinity binding pose does not necessarily have to be the catalytically active pose. For these reasons, we have performed the distance analysis not only for the first ranked pose, but we also present the shortest distance between the heme iron atom and the substrate's SOM when considering the five highest ranked poses or all 10 generated poses in a docking experiment (see Table 1).

Ligand Probing of the Binding Sites (LPBS). We want to emphasize that the effects of conformational changes of the protein will depend on both the exact region in the protein that is modified and the substrate under consideration. Therefore, a characterization of the conformational changes in terms of an atom-positional root-mean-square deviation (rmsd) after superposition will not reflect the chances in the docking results. Rather, we calculate the root-mean-square distance between the structural features of a set of substrates when docked to two protein structures. To describe the structural differences between two protein structures, we assign to each of the 65 substrates a value of 1 if the SOM lies within 6 Å of the heme iron atom and a value of 0 otherwise. The ligands probed binding site (LPBS) distance between the two protein structures is now expressed as the rmsd over the 65 assignments in both proteins. Similarly, the LPBS distance between two ensembles is calculated using the percentage of structures in which the substrates are successfully docked. The LPBS distance truly reflects the conformational changes of the protein that make a difference for this set of substrates. Of course, any structural feature may be used to calculate such a LPBS distance.

Decision-Tree Classification. The quality of the predictions of the SOM of substrates varies strongly between the different ensembles of protein structures and between the individual protein structures involved. In order to be able to predict the SOM for new putative substrates, it is highly advantageous if the ensemble or protein structure that most likely leads to the correct prediction could be determined *a priori*. For the 65 substrates under consideration here, the major SOM is known, and we can easily determine which ensemble or individual protein structure is most successful in predicting its SOM. We have used this information to train a decision tree using QSAR classification with 2-fold cross-validation as implemented in MOE. Our database of 65 substrates was randomly divided into two mutually exclusive subsets of size 33 (learning set) and 32 substrates (test set). As initial set of descriptors, we have considered the number of atoms, hydrophobic atoms, hydrogen atoms, halogens, rings, hydrogen bond acceptors, and hydrogen bond donors, as well as SlogP, molecular volume, total hydrophobic surface area, water-accessible surface area, weight, water-accessible surface area divided by the weight, and the first, second, and third kappa shape indexes (Kier 1, Kier 2, Kier 3).[35] Several decision trees were generated at different reliability levels and complexity. To avoid overfitting, only classification trees of depth 1 or 2 were considered. In the end the most simple, robust decision tree was selected (Figure 6), which was valid for both the selection of the best performing ensemble of protein structures (from a selection of the three essential ensembles) and for the selection of the best performing protein structures (from a selection of the three essential structures).

Acknowledgment. We gratefully acknowledge financial support from The Netherlands Organization for Scientific Research, Horizon Breakthrough grant 935.18.018 (JH) and VENI Grant 700.55.401 (CO).

Supporting Information Available: Figures of 65 substrates, with indications of their SOM, clustered into six groups; tables containing the docking results averaged over the 10 protein structure ensembles; substrates reclustered according to SOM predictions into ensembles and into single protein structures; and force field parameters for the representative substrates. This material is available free of charge via the Internet at http://pubs.acs.org.

References

(1) Ortiz de Montellano, P. R. *Cytochrome P450: Structure, Mechanism, and Biochemistry*, 3rd ed.; Kluwer Academic/Plenum Publishers: New York, 2005.

(2) Williams, J. A.; Hyland, R.; Jones, B. C.; Smith, D. A.; Hurst, S.; Goosen, T. C.; Peterkin, V.; Koup, J. R.; Ball, S. E. Drug-drug interactions for UDP-glucuronosyltransferase substrates: A pharmacokinetic explanation for typically observed low exposure (AUC(i)/AUC) ratios. *Drug Metab. Dispos.* **2004**, *32*, 1201–1208.
(3) Bazeley, P. S.; Prithivi, S.; Struble, C. A.; Povinelli, R. J.; Sem, D. S. Synergistic use of compound properties and docking scores in neural network modeling of CYP2D6 binding: Predicting affinity and conformational sampling. *J. Chem. Inf. Model.* **2006**, *46*, 2698–2708.
(4) Rendic, S. Summary of information on human CYP enzymes: Human P450 metabolism data. *Drug Metab. Rev.* **2002**, *34*, 83–448.
(5) Pirmohamed, M.; Park, B. K. Cytochrome P450 enzyme polymorphisms and adverse drug reactions. *Toxicology* **2003**, *192*, 23–32.
(6) Ingelman-Sundberg, M. Pharmacogenetics of cytochrome P450 and its applications in drug therapy: The past, present and future. *Trends Pharmacol. Sci.* **2004**, *25*, 193–200.
(7) de Groot, M. J.; Kirton, S. B.; Sutcliffe, M. J. In silico methods for predicting ligand binding determinants of cytochromes P450. *Curr. Top. Med. Chem.* **2004**, *4*, 1803–1824.
(8) De Graaf, C.; Vermeulen, N. P. E.; Feenstra, K. A. Cytochrome P450 in silico: An integrative modeling approach. *J. Med. Chem.* **2005**, *48*, 2725–2755.
(9) Stjernschantz, E.; Vermeulen, N. P. E.; Oostenbrink, C. Computational prediction of drug binding and rationalisation of selectivity towards cytochromes P450. *Expert Opin. Drug Metabol. Toxicol.* **2008**, *4*, 513–527.
(10) de Graaf, C.; Oostenbrink, C.; Keizers, P. H. J.; van Vugt-Lussenburg, B. M. A.; van Waterschoot, R. A. B.; Tschirret-Guth, R. A.; Commandeur, J. N. M.; Vermeulen, N. P. E. Molecular modeling-guided site-directed mutagenesis of cytochrome P450 2D6. *Curr. Drug Metab.* **2007**, *8*, 59–77.
(11) Rowland, P.; Blaney, F. E.; Smyth, M. G.; Jones, J. J.; Leydon, V. R.; Oxbrow, A. K.; Lewis, C. J.; Tennant, M. G.; Modi, S.; Eggleston, D. S.; Chenery, R. J.; Bridges, A. M. Crystal structure of human cytochrome P450 2D6. *J. Biol. Chem.* **2006**, *281*, 7614–7622.
(12) Guengerich, F. P. A malleable catalyst dominates the metabolism of drugs. *Proc. Natl. Acad. Sci. U.S.A.* **2006**, *103*, 13565–13566.
(13) Ekroos, M.; Sjogren, T. Structural basis for ligand promiscuity in cytochrome P450 3A4. *Proc. Natl. Acad. Sci. U.S.A.* **2006**, *103*, 13682–13687.
(14) Pang, Y. P.; Kozikowski, A. P. Prediction of the binding-sites of huperzine-A in acetylcholinesterase by docking studies. *J. Comput.-Aided Mol. Des.* **1994**, *8*, 669–681.
(15) Ma, B. Y.; Shatsky, M.; Wolfson, H. J.; Nussinov, R. Multiple diverse ligands binding at a single protein site: A matter of pre-existing populations. *Protein Sci.* **2002**, *11*, 184–197.
(16) Carlson, H. A. Protein flexibility and drug discovery: How to hit a moving target. *Curr. Opin. Chem. Biol.* **2002**, *6*, 447–452.
(17) Cruciani, G.; Carosati, E.; De Boeck, B.; Ethirajulu, K.; Mackie, C.; Howe, T.; Vianello, R. MetaSite: Understanding metabolism in human cytochromes from the perspective of the chemist. *J. Med. Chem.* **2005**, *48*, 6970–6979.
(18) Afzelius, L.; Arnby, C. H.; Broo, A.; Carlsson, L.; Isaksson, C.; Jurva, U.; Kjellander, B.; Kolmodin, K.; Nilsson, K.; Raubacher, F.; Weidolf, L. State-of-the-art tools for computational site of metabolism predictions: Comparative analysis, mechanistical insights, and future applications. *Drug Metab. Rev.* **2007**, *39*, 61–86.
(19) Ito, Y.; Kondo, H.; Goldfarb, P. S.; Lewis, D. F. V. Analysis of CYP2D6 substrate interactions by computational methods. *J. Mol. Graphics Model.* **2008**, *26*, 947–956.
(20) Saraceno, M.; Coi, A.; Bianucci, A. M. Molecular modelling of human CYP2D6 and molecular docking of a series of ajmalicine- and quinidine-like inhibitors. *Int. J. Biol. Macromol.* **2008**, *42*, 362–371.
(21) Lussenburg, B. M. A.; Keizers, P. H. J.; De Graaf, C.; Hidestrand, M.; Ingelman-Sundberg, M.; Vermeulen, N. P. E.; Commandeur, J. N. M. The role of phenylalanine 483 in cytochrome P450 2D6 is strongly substrate dependent. *Biochem. Pharmacol.* **2005**, *70*, 1253–1261.
(22) De Graaf, C.; Oostenbrink, C.; Keizers, P. H. J.; Van der Wijst, T.; Jongejan, A.; Vermeulen, N. P. E. Catalytic site prediction and virtual screening accuracy of cytochrome P450 2D6 substrates by consideration of water and rescoring in automated docking. *J. Med. Chem.* **2006**, *49*, 2417–2430.
(23) Molecular Operating Environment, v., Chemical Computing Group, Montreal, Canada.
(24) Christen, M.; Hunenberger, P. H.; Bakowies, D.; Baron, R.; Burgi, R.; Geerke, D. P.; Heinz, T. N.; Kastenholz, M. A.; Krautler, V.; Oostenbrink, C.; Peter, C.; Trzesniak, D.; Van Gunsteren, W. F. The GROMOS software for biomolecular simulation: GROMOS05. *J. Comput. Chem.* **2005**, *26*, 1719–1751.
(25) van Gunsteren, W. F.; Billeter, S. R.; Eising, A. A.; Hünenberger, P. H.; Krüger, P.; Mark, A. E.; Scott, W. R. P.; Tironi, I. G. *Biomolecular simulation: The GROMOS96 manual and user guide*, Vdf Hochschulverlag AG an der ETH Zürich: Zürich, 1996.
(26) Schuler, L. D.; Daura, X.; van Gunsteren, W. F. An improved GROMOS96 force field for aliphatic hydrocarbons in the condensed phase. *J. Comput. Chem.* **2001**, *22*, 1205–1218.
(27) Ryckaert, J.-P.; Ciccotti, G.; Berendsen, H. J. C. Numerical integration of cartesian equations of motion of a system with constraints: Molecular dynamics of n-alkanes. *J. Comput. Phys.* **1977**, *23*, 327–341.
(28) Hockney, R. W. The potential calculations and some applications. *Methods Comput. Phys.* **1970**, *9*, 136–211.
(29) Berendsen, H. J. C.; Postma, J. P. M.; van Gunsteren, W. F.; Hermans, J. Interaction models for water in relation to protein hydration. In *Intermolecular Forces*, Pullman, B., Ed.; Reidel: Dordrecht, The Netherlands, 1981; pp 331−342.
(30) Berendsen, H. J. C.; Postma, J. P. M.; van Gunsteren, W. F.; DiNola, A.; Haak, J. R. Molecular-dynamics with coupling to an external bath. *J. Chem. Phys.* **1984**, *81*, 3684–3690.
(31) Tironi, I. G.; Sperb, R.; Smith, P. E.; van Gunsteren, W. F. A generalized reaction field method for molecular-dynamics simulations. *J. Chem. Phys.* **1995**, *102*, 5451–5459.
(32) Jones, G.; Willett, P.; Glen, R. C.; Leach, A. R.; Taylor, R. Development and validation of a genetic algorithm for flexible docking. *J. Mol. Biol.* **1997**, *267*, 727–748.
(33) Eldridge, M. D.; Murray, C. W.; Auton, T. R.; Paolini, G. V.; Mee, R. P. Empirical scoring functions 0.1. The development of a fast empirical scoring function to estimate the binding affinity of ligands in receptor complexes. *J. Comput.-Aided Mol. Des.* **1997**, *11*, 425–445.
(34) Kirton, S. B.; Murray, C. W.; Verdonk, M. L.; Taylor, R. D. Prediction of binding modes for ligands in the cytochromes P450 and other heme-containing proteins. *Proteins: Struct., Funct., Bioinf.* **2005**, *58*, 836–844.
(35) Hall, L. H.; Kier, L. B. The molecular connectivity chi indices and kappa shape indices in structure-property modeling. In *Reviews in Computational Chemistry*, 2nd ed.; Lipkowitz, K. B.; Boyd, D. B., Eds.; VCH Publishers: New York, 1991; p 367.

JM801005M